Polymer Chemistry

ROYAL SOCIETY OF CHEMISTRY

PAPER

View Article Online
View Journal | View Issue

Cite this: *Polym. Chem.*, 2023, **14**, 303

How does the polymer architecture and position of cationic charges affect cell viability?†

Joana S. Correia, [a] Sofía Mirón-Barroso,[a] Charlotte Hutchings,[a] Silvia Ottaviani, [b,c] Birsen Somuncuoğlu, [a] Leandro Castellano,[c,d] Alexandra E. Porter, [a] Jonathan Krell [e] and Theoni K. Georgiou *[a]

Received 2nd August 2022,
Accepted 6th December 2022

DOI: 10.1039/d2py01012g

rsc.li/polymers

Polymer chemistry, composition and molar mass are factors that are known to affect cytotoxicity, however the influence of polymer architecture has not been investigated systematically. In this study the influence of the position of the cationic charges along the polymer chain on cytotoxicity was investigated while keeping constant the other polymer characteristics. Specifically, copolymers of various architectures, based on a cationic pH responsive monomer, 2-(dimethylamino)ethyl methacrylate (DMAEMA) and a non-ionic hydrophilic monomer, oligo(ethylene glycol)methyl ether methacrylate (OEGMA) were engineered and their toxicity towards a panel of cell lines investigated. Of the seven different polymer architectures examined, the block-like structures were less cytotoxic than statistical or gradient/tapered architectures. These findings will assist in developing future vectors for nucleic acid delivery.

1. Introduction

Polymers have been the focus of non-viral gene delivery methods for over three decades.[1–3] Their attractiveness in the field is a consequence of: (i) their ease of synthesis, (ii) the availability of monomers which allows for numerous combinations to be made when designing polymers, thus enabling the integration of key characteristics in one polymer chain and (iii) their ability to be further functionalised with targeting or imaging moieties through post-polymerisation methods.[3–6] Of the various polymer-based options available, cationic polymers have taken centre stage as their pH-dependent positive charges (amino groups), which can become protonated, enable interactions with the negatively-charged nucleic acids and cellular membranes. However, these same charges are the main contributors to the toxicity of cationic polymers that ultimately hinders their application as nucleic acid delivery systems.[7,8] These cationic charges are postulated to interact with phosphate groups on the cell membranes, destabilising them and causing cell toxicity.[9]

Polyethylenimine (PEI) and poly[2-(dimethylamino)ethyl methacrylate] (PDMAEMA) are the most studied cationic polymers for delivery of nucleic acids, closely followed by poly (amidoamine) (PAAs), poly-L-lysine (PLL), polylactic-*co*-glycolic acid (PLGA) and poly(β-aminoesters).[10–14] Of these, PEI was one of the first polymers reported as a DNA carrier in gene delivery studies,[15–18] which has branded this polymer as the "gold standard" for polymer-based delivery. PEI's commercial availability, high cationic charge density, efficient packaging of nucleic acids and high transfection rates are all contributors to its widespread use. Nonetheless, PEI's unacceptable cytotoxicity has been well documented.[8,19]

Similarly, DMAEMA based polymers have shown success in nucleic acid delivery, however data on its toxicity to cells is ambiguous, which has slowed down its translation into the clinic.[20–25] DMAEMA has a tertiary amine group, thus a less dense cationic character than PEI, which could attenuate toxicity and could be further diminished when coupled with other monomers that balance charge effects. What it is broadly accepted across the field is that there exists a clear trade-off between delivery (consequently, transfection efficiency) and cytotoxicity of polymers, which has led to continuous research efforts to adjust the balance, alleviate the latter and increase the former.[3]

One of the most common ways to improve cationic polymer cytotoxicity is to integrate poly(ethylene glycol) (PEG) – a neutrally charged, hydrophilic polymer – into the polymer chain.[26] PEG is well known for its biocompatibility and increasing

[a]*Department of Materials, Imperial College London, London, UK. E-mail: t.georgiou@imperial.ac.uk*
[b]*The John van Geest Cancer Research Centre, School of Science and Technology, Nottingham Trent University, Nottingham NG11 8NS, UK*
[c]*Department of Surgery and Cancer, Division of Cancer, Imperial College London, Imperial Centre for Translational and Experimental Medicine (ICTEM), London W12 0NN, UK*
[d]*School of Life Sciences, John Maynard Smith Building, University of Sussex, Brighton, UK*
[e]*Department of Surgery & Cancer, Imperial College London, UK*
† Electronic supplementary information (ESI) available. See DOI: https://doi.org/10.1039/d2py01012g

circulation times and is used in many FDA-approved products.[27,28] However, studies suggest that the mechanism by which the shielding effect of PEG chains limits undesirable interactions with negatively charged blood components and cell membranes,[29–32] also influences how the cationic charges from the polymer interact with nucleic acids, effectively decreasing cellular uptake, endosomal escape and consequently, molecule-delivery.[28,33]

Polymer characteristics, other than chemistry, have also been found to affect transfection efficiency and cytotoxicity. Early studies by Mikos's *et al.*[34] found that as molecular mass (MM) increased, so did the transfection efficiencies of PEI-based polyplexes into endothelial cells. However, their work did not investigate the toxicity of these polymers and there is evidence that polymer MM is inversely associated with cell viability.[8,19,35] Monnery *et al.*[8] investigated a range of linear and branched PEI and PLL-based polymers on a lung carcinoma cell line and found that higher MMs led to low cell viability caused by an increase in cell membrane damage. This trend was also observed on 3D structures[36,37] using star-shaped polymers for gene delivery; when MM was kept constant and monomer position was varied, gene delivery was improved, suggesting a role that polymer architecture plays in gene delivery systems.

Polymer architecture can be split into two categories: the position of the monomer in the polymer chain, and topology. In the case of topology, polymers can be further classified into linear, branched, graft or star-shaped architectures, depending on the spatial arrangement that the linear co- or homopolymers follow.[3,38,39] It is well established that stars outperform their linear counterparts or even branched/linear PEI in terms of toxicity, as well as nucleic acid complexation.[24,25,40–42] Additionally, the success of grafted structures is dependent on the content and composition of its side chains.[43] In fact, the flexibility warranted by the 3D conformation of branched and hyperbranched copolymers may improve interactions with the cell surface to reduce toxicity.[8,44,45]

In contrast to topology, the position of the monomers in the polymer chain has not been investigated systematically. Polymers are classed as homopolymers or as block-, gradient- or statistical copolymers,[4] in regard to monomer position. Linear architectures are the most studied for non-viral gene delivery vectors, however two points need to be clarified before they are developed. Firstly the effect of monomer position on cytotoxicity or cellular uptake is a controversial topic.[6,46–48] Second, there is little consistency between the experimental conditions: monomers, composition, molecular weight, linear *versus* non-linear architectures and synthetic method used, and also cell lines investigated across different studies to draw valuable conclusions about which parameters influence delivery. Alhoranta *et al.*[46] found that architecture does not affect cell viability in retinal cells by comparing linear and star DMAEMA-based copolymers. However, neither the MM nor the compositions of the polymers investigated were held constant and these factors impact cellular response. Bryer and colleagues[47] investigated triblock copolymers of poly((ethylene glycol) methyl ether methacrylate (OEGMA) and DMAEMA monomers copolymerised with a 2-(diethylamino)ethyl methacrylate and butyl methacrylate (DEAEMA-*co*-BuMA) copolymer. Their study found that monomer position did not affect cytotoxicity in immune cell lines, however the length of the OEGMA segment varied in the 6 polymers investigated. Perrier's[48] investigated triblock and statistical terpolymers with comparable MM and compositions, on cervical cancer cells (HeLa) and found that although monomer position did not impact cytotoxicity or cellular uptake in the long-term, the statistical polymer was internalised more rapidly than the block structures. In contrast, when statistical and diblock glycopolymers of 3.2 to 29.5 kDa were compared, statistical glycopolymers outperformed their corresponding diblocks in terms of cell survival and transfection efficiency.[6]

Nonetheless, cationic homopolymers generally show high transfection efficiencies, as the availability of charges allows for tight complexation of nucleic acids, however this is often accompanied by very high toxicity,[31,49,50] which explains the shift in the field towards more complex architectures and topologies.

Together, the literature suggests that the influence of parameters such as monomers used, hydrophobic content, charge density, molar mass or architecture on toxicity may be multifactorial rather than individual. Nonetheless it is important to understand individual trends to improve the design of polymeric delivery systems. Here we investigated 7 linear copolymers with varied architectures across five cell lines (two non-malignant control cell lines, human embryonic kidney 293 cells, HEK-293, and human pancreatic ductal cells, HPNE; and three pancreatic ductal adenocarcinoma (PDAC) cell lines, BxPC-3, PANC-1 and S2-007). All polymers had the same targeted MM and composition as both factors affect transfection and toxicity but varying position of the monomers withing the polymer chain (architecture). Specifically, copolymers of varying architectures (AB diblock, ABA triblock, BAB triblock, ABAB tetrablock, statistical, A-*b*-(A-*co*-B)-*b*-B and gradient/tapered copolymers) were synthesised through Group Transfer Polymerisation (GTP), using DMAEMA and oligo(ethylene glycol) methyl ether methacrylate (OEGMA molar mass = 300 g mol^{-1}) monomers. The physicochemical properties and influence of the panel of copolymers on cell viability were compared; the comonomer composition and the polymer molar mass were kept constant throughout. To the best of our knowledge this is the first study of its kind comparing multiple linear copolymers to evaluate the effect of architecture in cell–material interactions, in which the defining features of molar mass and composition were kept constant.

2. Experimental

2.1. Materials

All chemicals involved in polymer synthesis, purification and characterisation were purchased from Sigma-Aldrich, UK except for *n*-hexane that was used for polymer precipitation

that was obtained from VWR Chemicals. These were: 2,2-diphenyl-1-picrylhydrazyl hydrate (DPPH, free radical inhibitor), basic aluminium oxide (Al_2O_3·KOH), calcium hydride (CaH_2, ≥90%), 2-(dimethylamino)ethyl methacrylate (DMAEMA, 98%), oligo(ethylene glycol) methyl ether methacrylate (OEGMA, MM: 300 g mol^{-1}, 94%), methyltrimethylsilyl dimethylketene acetal (MTS, 95%), anhydrous tetrahydrofuran (THF, inhibitor-free, HPCL grade ≥99.9%), deuterated chloroform (chloroform-*d*, $CDCl_3$), poly(methyl methacrylate) (PMMA) standard samples (MM = 2000, 4000, 8000, 20 000, 50 000, 100 000 g mol^{-1}), branched polyethylenimine (PEI, MM by LS 25 000 g mol^{-1}), thiazolyl blue tetrazolium bromide reagent (MTT) and dimethyl sulfoxide (DMSO) Poly(tetrafluoroethylene (PTFE) hydrophilic syringe filters (0.45 μm pore size, 13 and 25 mm diameter), and nylon syringe filters (0.45 μm pore size, 25 mm diameter) were obtained from Thermo Fisher Scientific.

Dulbecco's modified Eagle's medium (DMEM) was obtained from Lonza. RPMI-1640 medium, foetal calf serum, L-glutamine, penicillin and streptomycin were obtained from Sigma-Aldrich, UK.

2.2. Purification of reagents

Ahead of synthesis, DMAEMA and OEGMA300 monomers were purified to remove inhibitors and acidic impurities. OEGMA300 was first diluted in THF in a 50 : 50 volume ratio and DMAEMA was used as provided. Both monomers were passed twice through basic aluminium oxide columns followed by the addition calcium hydride to remove any traces of humidity. For further purification, DMAEMA was freshly distilled under vacuum (after DPPH was added) the day before polymer synthesis. Due to its high molar mass, OEGMA300 was not distilled, but directly filtered into the reaction flask, similarly to Vamvakaki *et al.*[51] MTS was also distilled under vacuum for purification. The catalyst, tetrabutylammonium bibenzoate (TBABB), was *in-house* synthesized, following the procedure reported by Dicker *et al.*[52]

2.3. Group transfer polymerisation (GTP)

All copolymers were synthesised *via* a sequential – one pot GTP synthesis, where each block takes approximately 15 minutes. As an example, the synthesis of diblock, $OEGMA_{16}$-*b*-$DMAEMA_{32}$ (P1, AB), is described. Approximately 10 mg of TBABB were added to a round-bottom flask which was sealed with a rubber septum and purged with argon. This was followed by the addition of anhydrous THF (60 mL), addition of MTS (0.55 mL, 0.47 g, 3 mmol), filtration of the first monomer, OEGMA300 (22.5 mL, 11.8 g, 40 mmol) in the reaction flask and injection of DMAEMA (12.5 mL, 11.8 g, 80 mmol). As the synthesis is an exothermic reaction, the temperature of the reaction was monitored and recorded. Upon temperature stabilisation, 15 minutes after the addition of each monomer, two samples of approximately 0.1 mL each were collected for ^{1}H NMR and GPC analysis. Copolymers with statistical or gradient central blocks (*i.e.* P5, P6 and P7) were synthesised as above for the first block, followed by the simultaneous addition of monomers for central blocks, and again as initially described for all blocks that followed. The difference between the P6 and the gradient P7 is that for the gradient it was ensured that the rate of addition of the two monomers was different so a gradient distribution of the two monomers on the polymer chain was achieved. The synthesised copolymers were recovered in *n*-hexane and dried under vacuum and at room temperature for at least a week.

2.4. Gel permeation chromatography (GPC)

Molar masses (MM) and molar mass distributions (dispersities, *Đs)* of all copolymers and precursors were determined by GPC. Samples were analysed using GPC (SECurity GPC System 1260 Infinity, Agilent Technologies). The flow rate at the time of calibration and of experimental sample analysis was 1 mL min^{-1} and the mobile phase used was THF with 5% Et_3N. Samples were prepared by dissolution in the same solvent as the mobile phase and filtered using 0.45 μm PTFE filters prior to analysis. The system was calibrated with six PMMA standards.

2.5. Proton nuclear magnetic resonance (^{1}H NMR) spectroscopy

^{1}H NMR was carried out for every sample collected during and at the end of synthesis using a Jeol 400 NMR Spectrometer. $CDCl_3$ was used as solvent.

2.6. Cloud points

Cloud points (CPs) of 1% w/w polymer solutions in PBS were determined *via* Ultraviolet–visible (UV–Vis) Spectroscopy. A Cary UV–Vis Compact Peltier Spectrometer (Agilent, UK) equipped with a temperature probe and stirring was used for analysis. Samples were heated at 1 °C increments and each temperature was held for 30 seconds for stabilisation. Measurements were acquired at 550 nm, and a blank cuvette with PBS was used as reference. The instrument determines the cloud point temperature as the temperature at which a 50% change in transmittance is observed. The instrument error is ±1 °C.

2.7. Potentiometric titrations

Polymer solutions prepared in DI water (1 w/w%) were titrated to determine the pK_a values of DMAEMA units. A pH meter (Hanna Instruments, UK) with a two-point calibration at pH 4 and pH 7 was used. The pK_a is determined as the pH at which 50% of the amino groups are protonated.

2.8. Dynamic light scattering (DLS)

The experimental hydrodynamic diameters of 1% w/w polymer solutions (prepared in PBS) were determined using a Zetasizer Nano ZSP (Malvern, UK) which collects scattered light at a backscatter angle of 173°. Samples were filtered using 0.45 μm nylon filters to remove dust and left to rest for 30 minutes to allow dispersion of any bubbles formed during filtration. Each sample was run three times after an equilibrium time of 120 seconds. Experimental results are compared with theoretical hydrodynamic diameters, where for all copolymers a random coil configuration was assumed. The theoretical hydrodynamic diameters were calculated following the equation:[53]

$$d_h = 2 \times \left(2 \times 2.20 \times \frac{DP_{OEGMA} + DP_{DMAEMA}}{3}\right) 1/2 \times 0.154\,nm.$$

The DP values were calculated from the experimental M_n values after polymer precipitation, obtained by GPC, and experimental composition values determined by ^{1}H NMR. For OEGMA300, it was considered that the length of ethylene glycol (EG) chains to be 1.5 of the length of the methacrylate.[54] OEGMA300 has 4.5 EG groups, thus 6.75 was added to the DP_{OEGMA} (1.5 × 4.5).

2.9. Zeta potential

A Zetasizer Nano ZSP (Malvern, UK) was used to determine surface potential 1% w/w polymer solutions (prepared in PBS). For all measurements, cuvettes were prepared according to manufacturer's instructions and samples were carefully loaded on to the cuvettes to avoid formation of air bubbles and left to equilibrate for 120 seconds. Each measurement run was performed 3 times. Results were reported as an average of the measurement runs.

2.10. Cell culture

HEK-293, PANC-1 and BxPC-3 cell lines were obtained from American Type Culture Collection, S2-007 were obtained from Dr Silvia Ottaviani (The John van Geest Cancer Research Centre, Nottingham Trent University) and HPNE were obtained from Dr Jonathan Krell (Department of Surgery & Cancer, Imperial College London). HEK-293, PANC-1 and S2-007 were maintained in DMEM and BxPC-3 were maintained in RPMI-1640 medium, at 37 °C and 5% CO_2 humidified environment (standard culture conditions). Both DMEM and RPMI-1640 media were supplemented with 10% foetal calf serum (FCS), 2 mM L-glutamine, 100 U mL^{-1} of penicillin and 100 mg mL^{-1} of streptomycin. HPNE were maintained in DMEM supplemented with 5% FCS, 10 ng mL^{-1} of human epidermal growth factor, 4 mM L-glutamine, 100 U mL^{-1} of penicillin and 100 mg mL^{-1} of streptomycin.

2.11. Cytotoxicity

For standard 24 h assay, cells were seeded in 96-well microplates at densities of 10 000 (BxPC-3), 8000 (PANC-1, S2-007 and HEK-293) or 6000 cells per well (HPNE). For 48 h assays, cell densities were reduced to avoid over-confluency at the time of assay. After 24 h, cells were treated with increasing concentrations of polymer solution and left to incubate for a further 24 h at standard culture conditions. MTT reagent was added to each well in a 1 : 10 dilution and incubated for 4 hours at 37 °C. Medium was aspirated and DMSO used to solubilise formed crystals. Absorbance was read at 560 nm using OPTImax microplate reader. Untreated cells, seeded under the same experimental conditions, were used as negative control (100% cell viability). PEI, for its known cytotoxicity, was used as positive control. Three independent experiments, with three replicate wells, were carried out for each cell line. Percentage cell viability of each treatment, relative to untreated controls, was calculated following the equation,

$$\%\text{Cell viability} = \frac{A_{560\,treated} - A_{560\,blank}}{A_{560\,control} - A_{560\,blank}} \times 100, \quad \text{where} \quad A_{treated}$$

refers to the absorbance readings of cells treated with solutions and $A_{control}$ refers to the absorbance readings of untreated cells (negative control).

Note that the polymer concentrations tested ranged from 25 to 500 μg mL^{-1}. This is quite a broad range and normally the concentrations used to delivery therapeutics are within the lower limits of this range. Please also note that the MTT assay measures metabolic activity of the cells. Reduced metabolic activity compared to control cells suggests cell death but it is not uncommon for increased metabolic activity to be observed that will result to % cell viability higher than 100%.

2.12. Statistical analysis

Statistical analysis was carried out using GraphPad Prism 9 (Prism, San Diego, USA). Zeta potential results were analysed using 2-way ANOVA and Tukey's multiple comparison tests. MTT assay results were analysed using 2-way ANOVA or Kruskal–Wallis, and Tukey's or Dunn's multiple comparison tests, respectively. A p-value of * <0.05 was considered significant.

3. Results and discussion

In this study, seven linear copolymers with the same target MM (10 000 g mol^{-1}), OEGMA300-DMAEMA composition (50–50% w/w) and varying architectures were synthesised *via* GTP. All copolymers were composed of hydrophilic OEGMA300 block(s) (A) and DMAEMA block(s) (B). Architectures synthesised were diblock (AB, P1), triblock (ABA, P2, BAB, P3), tetrablock (ABAB, P4), statistical (A*co*B, P5), statistical-central block (P6, A-(A*co*B)-B) and gradient copolymer (A*grad*B, P7). The structures are schematically represented in Fig. 1, where OEGMA300 and DMAEMA units are represented in light green and dark blue spheres, respectively.

3.1. Molar mass and composition

Successful synthesis of all copolymers was monitored *via* GPC and ^{1}H NMR spectroscopy. Specifically, the MMs and compositions for all final polymers but for their precursors was determined and presented in Table 1. The final M_ns varied between 9400 and 12 200 g mol^{-1} (Table 1). The discrepancies between target and final M_n values can be explained by the deactivation of MTS molecules that are added to the active polymer chains, leading to higher experimental MM values, which have been reported in GTP.[55,56] Dispersity ($Đ$) (molar mass distribution) values vary between 1.10 and 1.20, and agree with previously reported values for copolymers synthesised through GTP and using OEGMA monomers.[57–60]

The GPC profile (Fig. 2) confirms the successful synthesis of polymer 1 (AB), $OEGMA300_{16}$-*b*-$DMAEMA_{32}$, and its precursor, with minimal deactivation. The progression of the reaction can be observed as the peak shifts towards higher MM values. The GPC traces of the copolymers followed a similar trend (Fig. S1†).

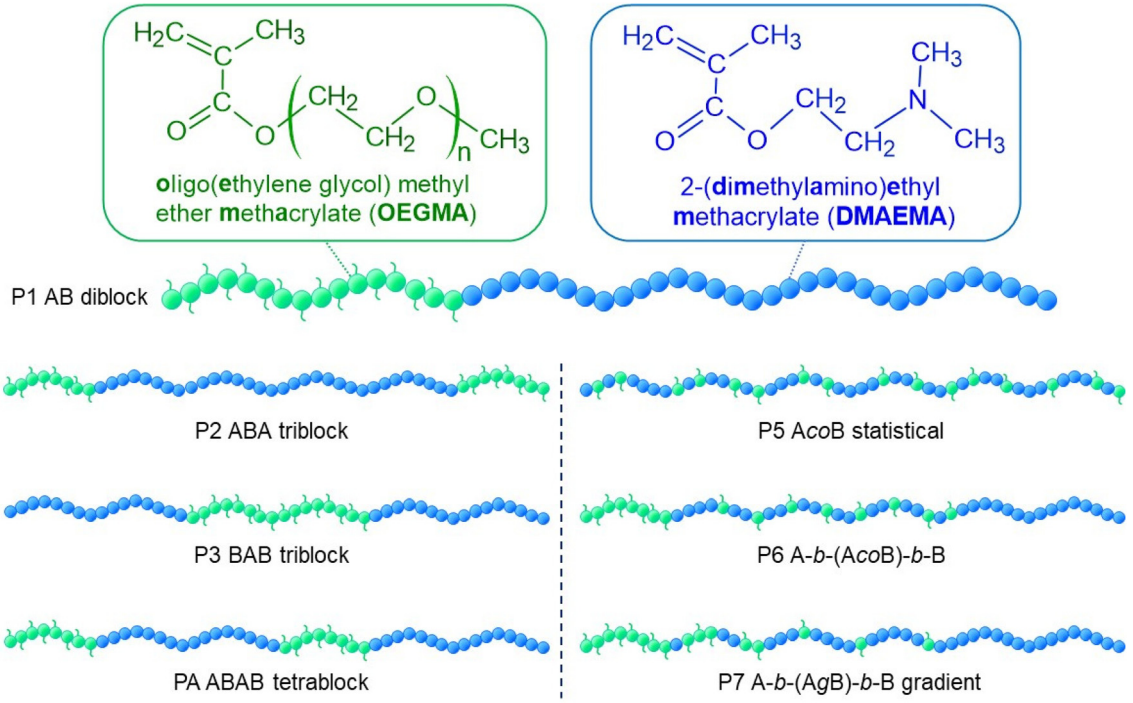

Fig. 1 Chemical structures and names of the monomers used in this study and a schematic representation of the architectures synthesised. OEGMA300 and DMAEMA units are represented in green and blue, respectively.

Table 1 Theoretical and experimental molar masses, distributions and compositions of the copolymers synthesised and their precursors

No.	Theoretical polymer structure[b]	$MM^{Theor.}$ [a] (g mol^{-1})	M_n (g mol^{-1})	$Đ$	w/w% OEG-DMA	
					Theor.	H^1 NMR
P1	OEG_{13}	4000	4300	1.16	100	100
	OEG_{13}-*b*-DMA_{25}	8100	10 113	1.10	50–50	49–51
P2	OEG_6	2000	3200	1.14	100	100
	OEG_6-*b*-DMA_{25}	6000	7600	1.17	64–36	64–36
	OEG_6-*b*-DMA_{25}-*b*-OEG_6	8100	11 800	1.14	50–50	56–44
P3	DMA_{12}	2000	2400	1.14	100	100
	DMA_{12}-*b*-OEG_{13}	6000	6200	1.17	66–34	66–34
	DMA_{12}-b-OEG_{13}-*b*-DMA_{12}	8100	9400	1.16	50–50	50–50
P4	OEG_6	2000	3000	1.16	100	100
	OEG_6-*b*-DMA_{12}	4000	5700	1.16	50–50	51–49
	OEG_6-*b*-DMA_{12}-*b*-OEG_6	6000	8300	1.18	66–34	66–34
	OEG_6-*b*-DMA_{12}-*b*-OEG_6-*b*-DMA_{12}	8100	11 500	1.20	50–50	49–51
P5	OEG_{13}-*co*-DMA_{25}	8100	11 200	1.19	50–50	51–49
P6	OEG_6	2000	3200	1.16	100	100
	OEG_6-*b*-(OEG_{12}-*co*-DMA_6)	6000	8200	1.19	66–34	65–35
	OEG_6-*b*-(OEG_{12}-*co*-DMA_6)-*b*-DMA_{12}	8100	12 200	1.20	50–50	50–50
P7	OEG_6	2000	2700	1.14	100	100
	OEG_6-*b*-(OEG_2-*grad*-DMA_1) #1	3000	3000	1.14	80–20	98–2
	OEG_6-*b*-(OEG_4-*grad*-DMA_2) #2	4000	3600	1.17	60–40	94–6
	OEG_6-*b*-(OEG_6-*grad*-DMA_7) #3	5000	4000	1.13	40–60	88–12
	OEG_6-*b*-(OEG_6-*grad*-DMA_{12}) #4	6000	7100	1.18	20–80	66–34
	OEG_6-*b*-(OEG_6-*grad*-DMA_{12})-*b*-DMA_{12}	8100	9400	1.18	50–50	50–50

[a] Theoretical MM ($MM^{theor.}$) was calculated using the equation: $MM^{theor.}$ (g mol^{-1}) = (Σ_i MM_i × DP_i) + 100, where MM_i and DP_i correspond to the MM of the monomer and its degree of polymerisation, respectively. The addition of 100 g mol^{-1} accounts for the mass of the initiator that remains on the polymer chain. [b] Abbreviated nomenclature. OEG and DMA refer to OEGMA and DMAEMA, respectively.

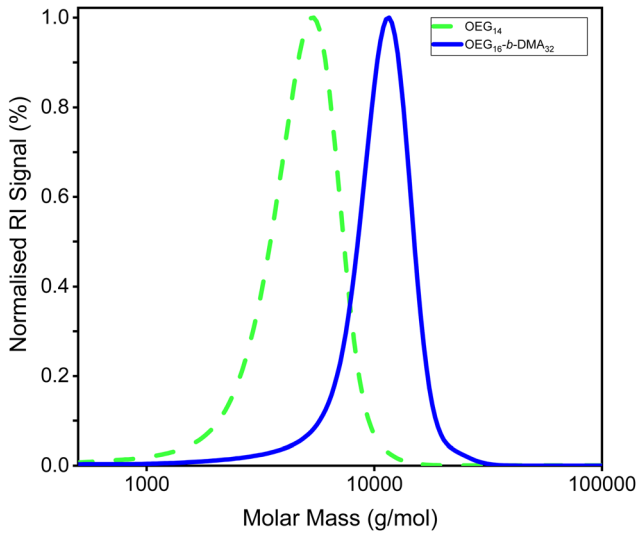

Fig. 2 GPC chromatogram of the AB diblock copolymer, $OEGMA300_{16}$-*b*-$DMAEMA_{32}$ (P1), and its precursor. $OEGMA300_{14}$ (abbreviated OEG_{14} on inset legend) and the final polymer (abbreviated OEG_{16}-*b*-DMA_{32} on inset legend) are represented by the green dashed line and blue solid line, respectively.

^{1}H NMR spectra of polymer 1 and its precursor is shown in Fig. 3. The three methoxy protons of OEGMA300, found next to the methyl group, are labelled "e" on Fig. 3, are represent the monomer distinct peak. For the second monomer, DMAMEMA, its peak is labelled "h" and distinguishes the 6 methyl protons next to the nitrogen atom. These two peaks were used to determine the composition of all polymers and their precursors. ^{1}H NMR spectra of copolymers P2–P7 can be found in the ESI (Fig. S6A–F†). Theoretical and experimental compositions were in agreement (Table 1), confirming successful synthesis for all copolymers.

3.2. Physicochemical properties

Properties such as pK_a, surface charge and size are known to influence cell–material interactions. Cloud point temperatures (CPs) were also determined to investigate the solubility of copolymer in aqueous solutions resembling physiological environment (37 °C, pH 7–7.4). All copolymers were found to be soluble in aqueous solvents, either DI water, sterile PBS and cell culture media, in agreement with the hydrophilic nature of both monomers used. For investigation of aqueous solution

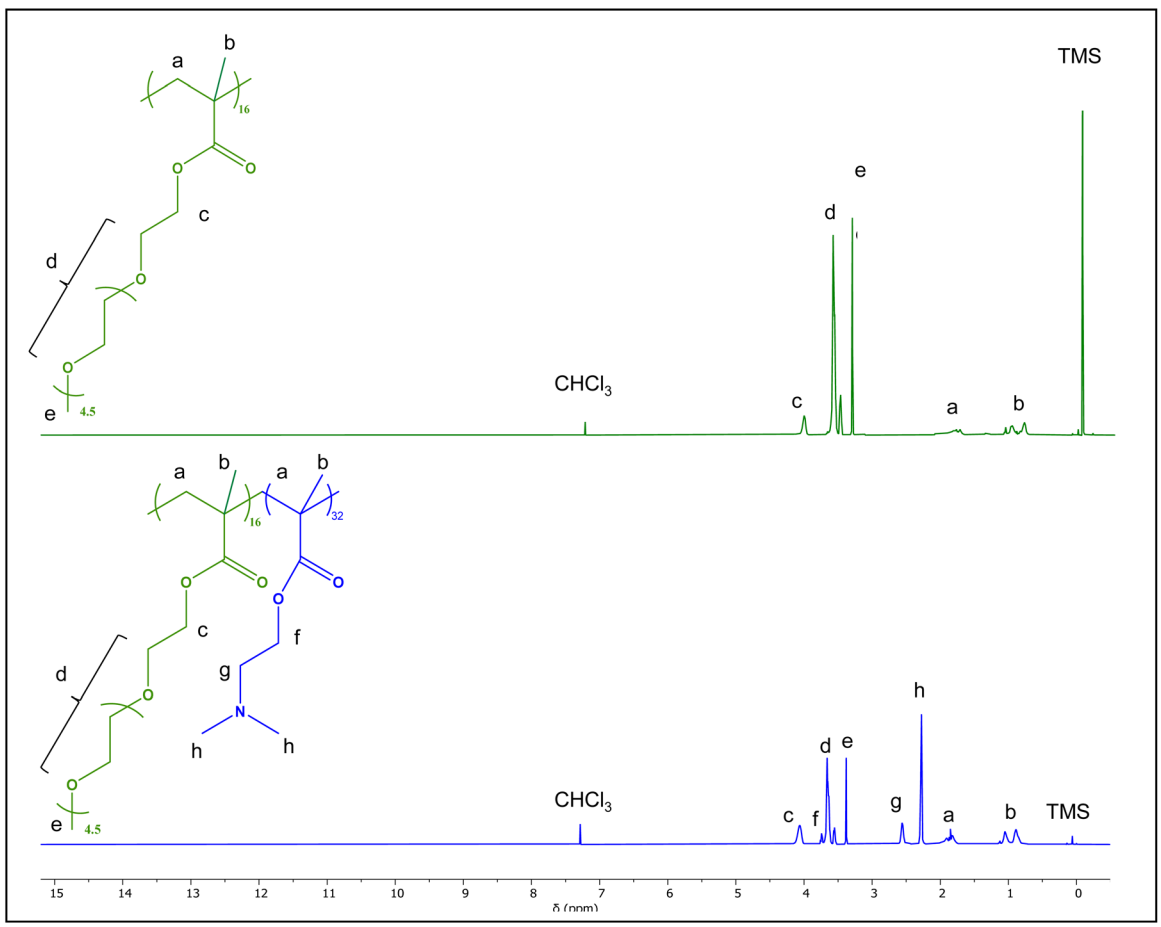

Fig. 3 H^1 NMR spectra of the AB diblock copolymer, $OEGMA300_{16}$-*b*-$DMAEMA_{32}$ (P1), and its precursor. The first block of the copolymer, OEGMA300, is represented in green (chemical structure and spectra), the second block, DMAEMA, is represented in bright blue (chemical structure), and the final spectra in bright blue.

properties, 1% w/w polymer solutions either in DI water or PBS were made unless stated otherwise.

3.2.1. Cloud points. The cloud point temperatures for all copolymers solutions (1 wt%) were determined at the solutions original pH, where most of the DMAEMA units are not protonated, and at physiological pH range, where around 50% of the DMAEMA units are protonated. Heat curves of each copolymer can be found on Fig. S7 (ESI†).

CPs are indicative of the hydrophilicity of polymers and consequently, their tendency for aggregation. DMAEMA homopolymers have an expected CP of around 50 degrees,[60,61] introducing a hydrophilic monomer, such as OEGMA in this case, will lead to an increase in cloud point temperatures, a trend described by others.[55,61–64] In this study, CPs ranged between 55 and 58 °C in a non-protonated state and no clear differences were observed between the different architectures. Additionally, since the amine groups of DMAEMA become protonated at physiological pH range, the polymer becomes even more hydrophilic,[65,66] which explains why no CPs were observed at pH = 7. As expected, PEI did not display a cloud point due to its higher charge density.

3.2.2. Size. Hydrodynamic diameter measurements were carried out at non-protonated and protonated states at 37 °C (Table 3, pH 9 and pH 7, respectively). Given the hydrophilic nature of both DMAEMA and OEGMA units, a random coil configuration was assumed for all copolymers and theoretical diameters were calculated following the equation $d_h = 2 \times \left(2 \times 2.20 \times \frac{DP_{OEGEMA} + DP_{DMAEMA}}{3}\right)1/2 \times 0.154\,\text{nm}$.

All copolymers were found to be nano-sized (D_H < 10 nm) and have narrow size distributions. At this size and considering the hydrophilic nature of DMAEMA and OEGMA, no self-assembly was expected and the polymers' chains are in the form of unimers. Mendrek and co-workers[24] report hydro-

Table 2 Architecture, theoretical structure, effective pK_a and cloud point temperatures (through visual and UV–Vis spectroscopy determination) of all copolymers synthesised and of PEI

				Cloud points (°C)	
				UV–Vis (±1)	
No.	Arch.	Theoretical polymer structure[a]	pK_a	pH 9[b]	pH 7[b]
P1	AB	OEG_{13}-*b*-DMA_{25}	7.4	56	N.D
P2	ABA	OEG_6-*b*-DMA_{25}-*b*-OEG_6	7.3	57	N.D
P3	BAB	DMA_{12}-*b*-OEG_{13}-*b*-DMA_{12}	7.3	56	N.D
P4	ABAB	OEG_6-*b*-DMA_{12}-*b*-OEG_6-*b*-DMA_{12}	7.1	55	N.D
P5	A*co*B	OEG_{13}-*co*-DMA_{25}	7.1	56	N.D
P6	A(A*co*)B	OEG_6-*b*-(OEG_{12}-*co*-DMA_6)-*b*-DMA_{12}	7.2	55	N.D
P7	A(A*grad*B)B	OEG_6-*b*-(OEG_6-*grad*-DMA_{12})-*b*-DMA_{12}	7.3	58	N.D
PEI	Branched	N.A	N.A	N.D	N.D

[a] Abbreviated nomenclature. OEG and DMA refer to OEGMA and DMAEMA, respectively. [b] pH 9 and pH 7 refer to approximated pH of solutions tested. The pH of each solution was measured before each experiment. On a non-protonated state, the copolymers solutions pH ranged from 8.7 to 9 for all copolymers. When protonated to physiological pH, values ranged from 7.0 to 7.2. For PEI, the solutions' pH prior to testing was found to be at 10.9 and 7.1, respectively. N.A – not applicable. Cannot be calculated. N.D – not determined. Cloud point temperature not found at the temperature range tested (21–80 °C).

Table 3 Architecture, theoretical structure, theoretical and experimental hydrodynamic diameters (by intensity) of copolymers synthesised and of PEI

			Hydrodynamic diameter[b] (D_H, nm, ±0.5)				
No	Arch.	Theoretical polymer structure[a]	Theor.[c]	pH 9[d]	PDI pH 9	pH 7[d]	PDI pH 7
P1	AB	OEG_{13}-*b*-DMA_{25}	2.8	5.6	0.146	4.9	0.127
P2	ABA	OEG_6-*b*-DMA_{25}-*b*-OEG_6	2.9	6.5	0.120	6.5	0.218
P3	BAB	DMA_{12}-*b*-OEG_{13}-*b*-DMA_{12}	2.7	4.9	0.220	5.6	0.120
P4	ABAB	OEG_6-*b*-DMA_{12}-*b*-OEG_6-*b*-DMA_{12}	3.0	5.6	0.086	5.6	0.312
P5	A*co*B	OEG_{13}-*co*-DMA_{25}	2.9	5.6	0.091	6.5	0.219
P6	A(A*co*)B	OEG_6-*b*-(OEG_{12}-*co*-DMA_6)-*b*-DMA_{12}	3.0	6.5	0.076	6.5	0.136
P7	A(A*grad*B)B	OEG_6-*b*-(OEG_6-*grad*-DMA_{12})-*b*-DMA_{12}	3.0	5.6	0.112	5.6	0.152
PEI	Branched	N.A	N.A	10.1	0.179	10.1	0.195

[a] Abbreviated nomenclature. OEG and DMA refer to OEGMA and DMAEMA, respectively. [b] The experimental hydrodynamic diameters reported are the average (of 3 independent runs) of the mean diameters of the maximum peak reported by the instrument. [c] Calculations for the theoretical diameters are based on the experimental degrees of polymerisation (DPs). DPs were calculated by using the experimental MM after precipitation, determined by GPC, and experimental composition, by ^{1}H NMR. Theoretical diameters assume a random coil configuration and were calculated following the equation:[53] $d_h = 2 \times \left(2 \times 2.20 \times \frac{DP_{OEGMA} + DP_{DMAEMA}}{3}\right)1/2 \times 0.154\,\text{nm}$. [d] pH 9 and pH 7 refer to approximated pH of solutions tested. The pH of each solution was measured before each experiment. On a non-protonated state, the copolymers solutions pH ranged from 8.7 to 9 for all copolymers. When protonated to physiological pH, values ranged from 7.0 to 7.2. N.A – not applicable. Cannot be calculated.

dynamic radius ranging between 10–14 nm for DMAEMA-OEGMA stars while Hong-Tan *et al.*[67] found ranges of 12–18 nm for hyperbranched DMAEMA-OEGMA statistical structures. It is of note that the MMs used in these studies are significantly different than those reported here, as expected since the hydrodynamic diameter increases with increasing MM.[24,25,40] At 37 °C results also show no evidence of self-aggregation in either protonation state, in agreement with the cloud point temperatures observed. However, it must be noted the difference between theoretical and experimental values is due to steric hindrance caused by the presence of EG side groups, which forces the polymer chain to be in a more extended configuration. As expected, PEI has a greater hydrodynamic diameter (of 10 nm) since it has a higher MM.

3.2.3. Effective pK_as. All copolymers had an acid dissociation constant (pK_a) values in the range of 7.1–7.4 (Table 2.) agreeing with previously described values for DMAEMA-based copolymers.[55,68,69] The pK_a of a polymer describes the pH at which 50% of its ionizable groups are in a protonated state, thus in environments where the pH is lower than the pK_a, there is an abundance of protons, and the pK_a can also be used to infer the polymer's charge under varying pH conditions.[70] The pK_a values reported indicate that the copolymers in this study are partially protonated at physiological pH, carrying a cationic charge.

3.2.4. Zeta potential. The surface charge of all copolymers in PBS was found to be moderately positive, with zeta potential values varying from 0.32 to 5.63 mV, at a physiological pH (Fig. 4). Based on the pK_a values reported, these results were anticipated, however they do not match the values of linear PDMAEMA (15 mV) or other DMAEMA-based polymers at non-protonated and protonated states.[24,70] Our data can be explained due to the shielding effect of the PEG-chains present in our copolymers, given the high OEGMA content.[28] Additionally, comparison with other studies is conflicting due to the sensitivity of zeta potential measurements to sample concentration, pH and ionic strength.[41,71] In contrast, branched PEI had a noticeably higher zeta potential of around +14.93 mV (±1.73 mV), which is in agreement with previously reported values and is explained by PEI's greater density of ionizable groups.[72] As charge and cytotoxicity are intrinsically related and recognising the marked toxicity of PEI in *in vitro* models, the lower zeta potential values reported for our copolymers could hint toward them being less cytotoxic. The significant differences found between the designed copolymers also suggest copolymers P5 to P7, non-block architectures (A*co*B, A-(A*co*B)-B and gradient, respectively) are potentially more cytotoxic than their block architecture counterparts (P1–P3). Tetrablock copolymer P4, ABAB, however, has slightly higher zeta potential though this difference was only significant in comparison to P1.

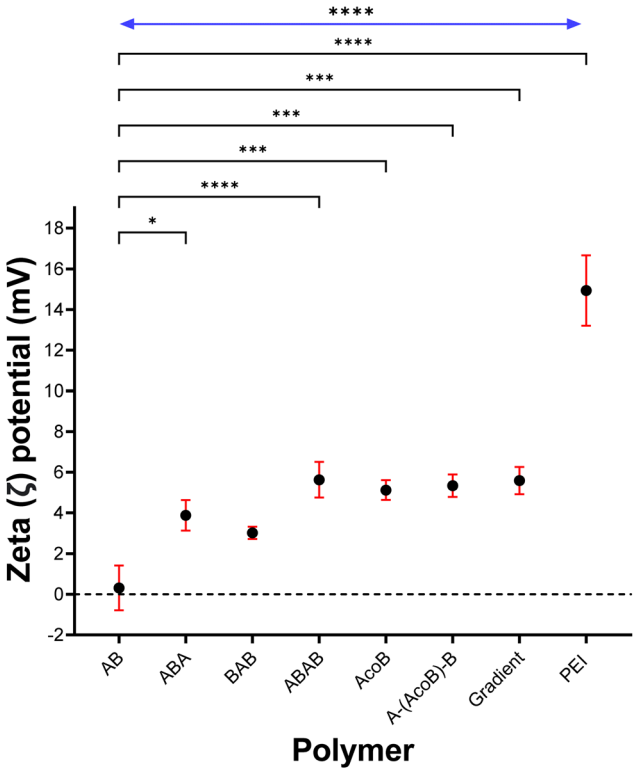

Fig. 4 Zeta potential (ζ, mV) of each copolymer and PEI at physiological pH (at 1 wt% in PBS). Results are shows as mean ± SEM (n = 9). Dotted line represents neutral surface charge (ζ = 0 mV). Significances denoted were investigated using a one-way ANOVA and Tukey's multiple comparisons test, where ****P < 0.0001, ***P < 0.001, **P < 0.01 and *P < 0.05. P-Values in bracket compare each architecture to copolymer AB (P1). Significance in arrow (top) was found to be the same for all copolymers, when compared to PEI.

4. Cytotoxicity

4.1. Non-malignant models

Cytotoxicity was investigated in HEK-293 (human embryonic kidney cells) and HPNE (human pancreatic ductal cells) cell lines as non-malignant models. MTT assay was used to measure metabolic activity of cells. Reduced metabolic activity correlates to cell toxicity or unhealthy cells. The cell viability percentages were calculated relative to untreated controls, most measurements observed for copolymers report a cell viability greater than 100%.[50]

MTT assay demonstrated a time, concentration and polymer dependent effect in cell viability, across all pancreatic cell lines. In HEK-293, significant differences were found between block-like and non-block architectures, at 24 hours (Fig. 5). Particularly, exposure to polymer P6, a statistical central block, lead to a reduction of up to 25% in cell viability at the three highest concentrations (125 μg mL^{-1}, 250 μg mL^{-1} and 500 μg mL^{-1}). Exposure to the gradient copolymer (P7) was only found significant, compared to the others, at 500 μg mL^{-1} with a reduction of 20% in cell viability. In contrast, block architectures were not found to impact cell viability significantly. No significant reduction in cell viability was measured for any of the copolymers, at 48 hours (Fig. S2†). The effects of other cationic polymers on the viability of HEK-293 cells and cell transfection has been described by others'.[44,71,72] Cook *et al.*[44] found bPEI to be cytotoxic at low

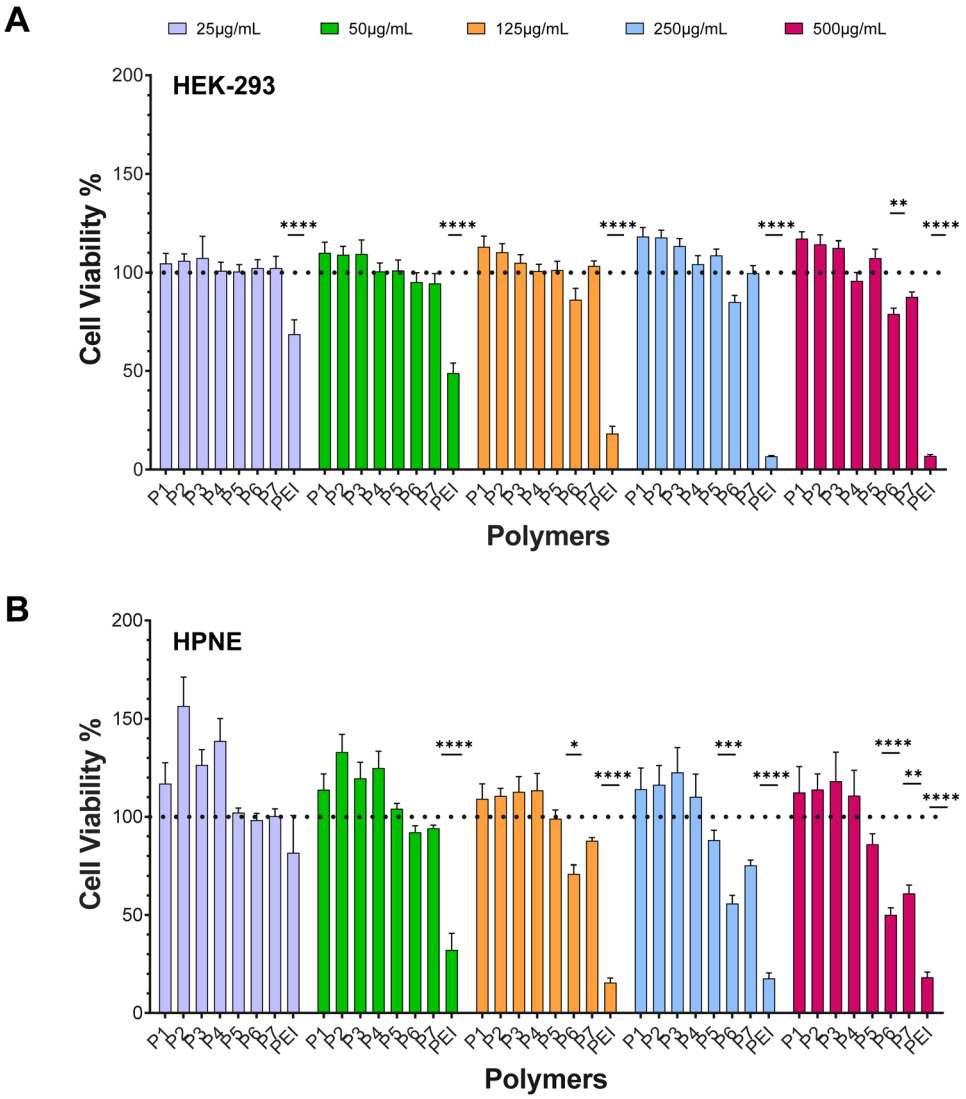

Fig. 5 Effect of monomer distribution on non-malignant cell lines. HEK-293 (A) and HPNE (B) were treated with increasing concentrations of polymer solutions for 24 hours. Polymer concentrations, for all copolymers, are: 25 µg mL^{-1} (lilac), 50 µg mL^{-1} (green), 125 µg mL^{-1} (orange), 250 µg mL^{-1} (blue) and 500 µg mL^{-1} (pink). Polymer abbreviations for P1 to P7 are AB, ABA, BAB, ABAB, AcoB, A(AcoB)B and gradient, respectively. PEI was used a positive control (cytotoxic). Cell viability is reported as percentage relative to untreated control cells (0 µg mL^{-1}, not plotted). Black dotted line indicates 100% cell viability (control). Data shown as mean ± SEM from triplicates. Differences in mean cell viability between polymers was investigated using Two-way ANOVA and Tukey's multiple comparison tests. Significance denoted ****$P < 0.0001$, ***$P < 0.001$, **$P < 0.01$, *$P < 0.05$.

concentrations (200 µg mL^{-1}), which was significantly improved with the introduction of a second monomer in poly (ethylenimine-*co*-oxazoline) copolymers. The copolymers transfection efficiency was roughly 25% lower than that of bPEI but with much reduced cytotoxic effects in HEK-293. Similarly, Yu[73] showed cell viability to decrease around 70% when exposed to 25 kDa PEI but only 15–20% with PDMAEMA linear polymers. Transfection efficiency was also remarkable compared to PEI, however it must be noted that such improvement could be due to the marked cell death caused by PEI exposure. In contrast, PDMAEMA polymers of Bitoque *et al.*[74] were cytotoxic towards HEK-293 cells in concentrations as low 10 µg mL^{-1}, but no decrease in cell viability was observed when their polymers were complexed with DNA. Together, these studies show that complexation limits the amount of charges available to disrupt the cellular membrane and cause toxicity, which translates in lower cytotoxic effects from polyplexes. Our results show a similar trend of polymer-only toxicity, which is a promising sign on the suitability of our copolymers for gene delivery.

Similarly, HPNE cells appeared to be more susceptible to non-block architectures. When exposed for 24 hours to P6 (A-(A*co*B)-B) and P7 (A(A*grad*B)B), copolymers of random (less-ordered) monomer distributions, a significant decrease in cell viability was observed (Fig. 5). Exposure to gradient copolymer led to a 30% decrease in cell viability at the highest concentration (500 µg mL^{-1}). A-(A*co*B)-B (P6) showed significant cytotoxic effects from a concentration of 125 µg mL^{-1} and higher,

with cell viability decreasing with concentration. A reduction of more than 50% in cell viability was observed for the two highest concentrations when exposed to A-(A*co*B)-B. By comparison with 24 hours, results show that longer exposure time to the polymer significantly impacts cell viability at lower concentrations. At 48 hours (Fig. S2†), exposure to A-(A*co*B)-B (P6) saw a 30% reduction in cell viability at lowest concentration (25 μg mL^{-1}) which doubled at highest concentration (60% reduction, 500 μg mL^{-1}). Exposure to P7 led to a 50% reduction at the highest concentration, *versus* 30% at 24 hours. Surprisingly, not having been observed at 24 hours, A*co*B (P5) 48 hours exposure reduced cell viability 20–40% as concentration increased from 50 μg mL^{-1}.

4.2. PDAC models

The cell viability of BxPC-3 and PANC-1 PDAC cell lines was significantly more affected by exposure to the statistical/tapered co-polymers (Fig. 6). For the BxPC-3 cells, non-block architectures P5, P6 and P7 were found to negatively impact cell viability. A*co*B (P5) led to a decrease in cell viability of more than 30% at the two highest concentrations investigated. A(A*co*B)B (P6) decreased cell viability between 30% and 60% from exposures as low as 50 μg mL^{-1}. Finally, cell viability was around 30% when exposed to the gradient copolymer at the highest concentration, which is nearly a 70% reduction. At 48 hours (Fig. S3†), however, cytotoxic effects were not observed which is unusual – increasing dosage and time of exposure normally leads to higher cytotoxicity. Our results suggest that cells recover after initial insult, however this was not observed (nor expected to) with the control PEI. Further studies will need to be performed to understand why this is observed and why metabolic activity seems to increases in some cases.

For PANC-1, while it seems that A-(A*co*B)-B, P6, could be affecting cell viability (Fig. 6) no significant differences were found compared to untreated cells. It was observed that as concentration increased, so did cell viability, which is unusual. A hallmark of cancer is that cells proliferate in excess partly due to a stress-induced response, in which if a given dosage does not induce cell death pathways, cells will continue to proliferate.[75,76] Considering that PEI, follows a standard trend in which cell viability is negatively impacted with increasing concentrations, the increase in cell viability observed for P6 is likely an artefactual result. At 48 h (Fig. S3†), while it was visually clear that copolymers P5, P6 and P7 to potentially have an effect on cell viability, following the same trend as positive control PEI, this was not found to be significant.

Similar to what was observed for PANC-1 cells, none of the architectures investigated were found to affect cell viability on the S2-007 cells, at either timepoint (Fig. 6 and Fig. S3†). While at 24 hours cell viabilities kept increasing with exposure to higher concentrations, at 48 hours (Fig. S3†), the opposite was observed and agrees with what has been previously described for the other cell lines in this study: that A(A*co*B)B and gradient copolymers may affect cell viability however, in this case, this was not found to be significant.

As PDAC models, the cells lines share genotypic profiles, such as mutations on KRAS and tumour suppressor genes TP53, SMAD4 and CDKN2a, which lead to a higher proliferative and invasiveness profile and to an inability to regulate cell division pathways, recognise DNA-damaged cells and induce cell death in such cases.[77–79] These mutations can play a role in the cytotoxicity resistance observed. On the other hand, the more pronounced cytotoxic effects observed in HPNE, could be due to opposite reasoning – the lack of mutations that allow evasion from cellular death pathways or promote stress-induced proliferative states.

In comparison with our copolymers, PEI's cytotoxicity increased with concentration, a trend well described in the literature across different cell lines[80–83] and mirrored by the results here described for both non-malignant and PDAC models. PEI's high density of cationic charges, as a result of primary, secondary and tertiary amines present, have been hypothesised to cause membrane disruption.[84]

4.3. Effect of architecture on cytotoxicity

As evidenced by the cytotoxicity results, copolymers in which cationic charges are randomly distributed across the chain show lower cell viability than those with cationic charges distributed in predetermined manner. These results were unexpected. Singhasa and co-workers[85] investigated a range of linear glycopolymers, of *N*-[3-(dimethylamino)propyl]methacrylamide hydrochloride copolymerised with methacrylamide hydrochloride, *N*-(3-aminopropyl) morpholine methacrylamide and 2-lactobionamidoethyl methacrylamide where having a statistical component led to better cell viability when compared with strictly block architectures. This was particularly relevant in copolymers carrying tertiary amines, which has been described in earlier studies and in copolymers of similar MM to those here described.[21,28,85] This trend has also been observed in more complex structures, where stars with arms of random distribution were found less toxic than diblock arms.[25] In contrast, comparing linear block copolymers of PDMAEMA-Poly(β-aminoesters) with PDMAEMA homopolymer, strengthens the evidence that higher accessibility of positive charges to interact with the cellular membrane leads to its disruption and consequently lower cell viability.[31,86,87]

It is conventionally accepted that cationic polymers interact with the cell membrane *via* non-specific electrostatic interactions.[3,88] This interaction between positive and negative charges is hypothesized to create holes in the cell membrane, which permeabilises it, thus improving cellular uptake, but can also lead to membrane destabilization, potentially initiating cell death pathways. Ruenraroengsak *et al.*[89] investigated alveolar epithelial cells exposed to amine-, carboxyl- and unmodified polystyrene nanoparticles of 50 nm in size. Live imaging analysis of cell topography found the formation of holes in the cell membrane as well as diminished cell membrane density, when exposed to amine-modified NPs (+50 mV) but not with the other formulations (−10 to −50 mV). Their results suggest that electrostatic interactions between amine groups and phospholipids of the lipid bilayer causes the for-

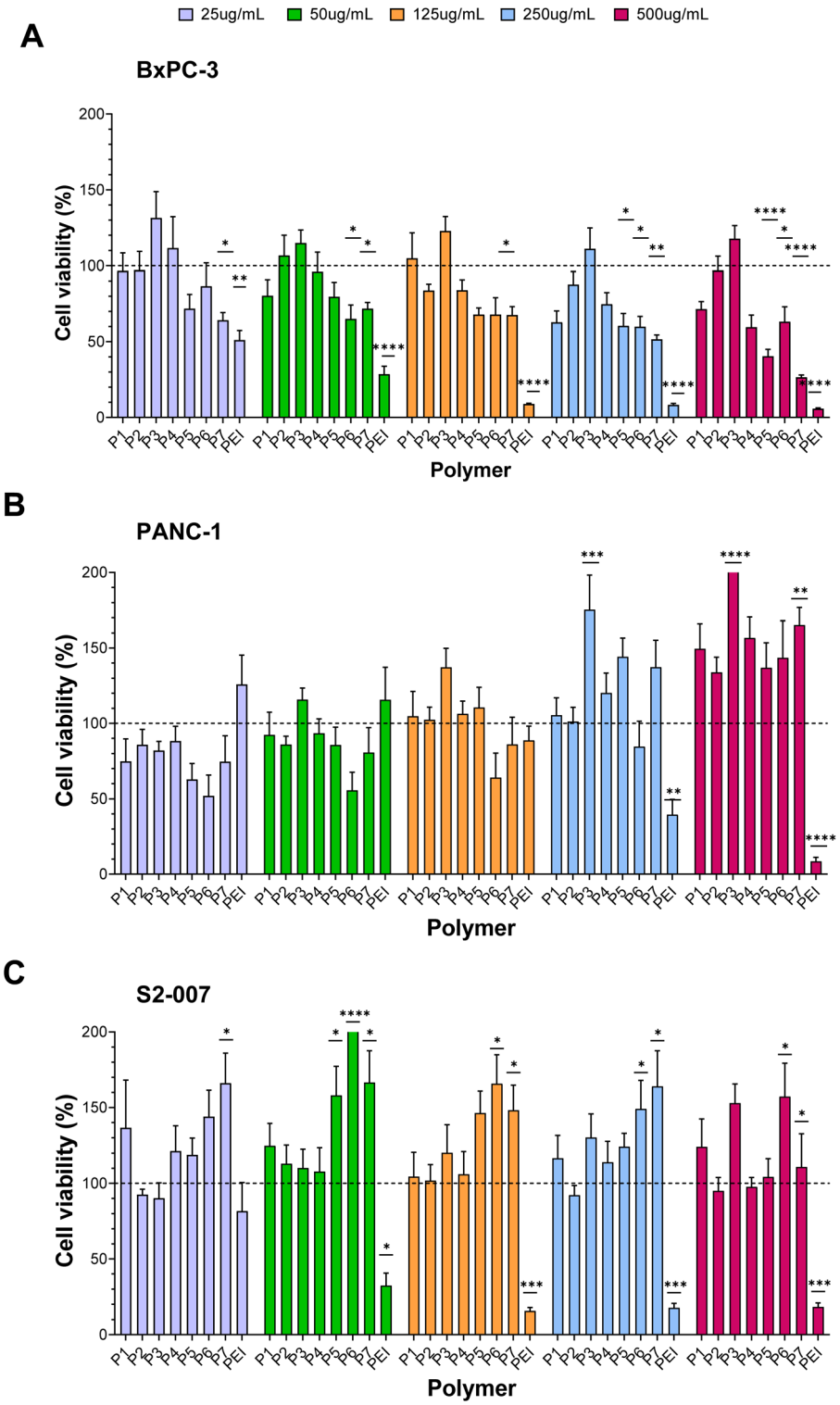

Fig. 6 Effect of monomer distribution on PDAC cell lines. BxPC-3 (A), PANC-1 (B) and S2-007 (C) cells were treated with increasing concentrations of polymer solutions for 24 hours. Polymer concentrations, for all copolymers, are: 25 μg mL^{-1} (lilac), 50 μg mL^{-1} (green), 125 μg mL^{-1} (orange), 250 μg mL^{-1} (blue) and 500 μg mL^{-1} (pink). Polymer abbreviations for P1 to P7 are AB, ABA, BAB, ABAB, A*co*B, A(A*co*B)B and gradient, respectively. PEI was used a positive control (cytotoxic). Cell viability is reported as percentage relative to untreated control cells (0 μg mL^{-1}, not plotted). Black dotted line indicates 100% cell viability (control). Data shown as mean ± SEM from triplicates. Differences in mean cell viability between polymers was investigated using Kruskal–Wallis tests and Dunn's multiple comparison testes. Significance denoted ****$P < 0.0001$, ***$P < 0.001$, **$P < 0.01$, *$P < 0.05$.

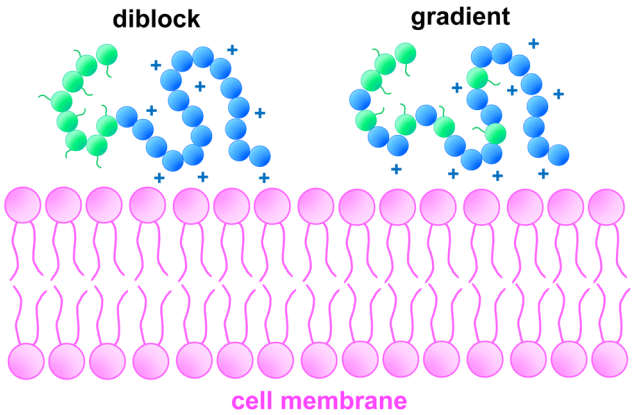

Fig. 7 Conceptual illustration of the effect of monomer distribution on cell membrane interaction. Blue sections represent partially protonated DMAEMA units, green sections represent other monomer units (in the case of this schematic, OEGMA300). A wider distribution of cationic charges may lead to a higher number of interactions with the negatively charged cellular membrane, disturbing the membrane across more locations, leading to increased toxicity.

mation of holes, as the lipid bilayer transitions into liquid phase. Ruenraroengsak *et al.*[89] shows the effect surface chemistry can have in cell–material interactions. This has also been described in poly(ethylenimines) by Monnery *et al.*[8] We further hypothesise that its location (*i.e.* of charged groups) within the polymer chain has distinct impact in cytotoxicity.

In the present study, we hypothesis that, because the cationic charges of the statistical or gradient copolymers are more spread out in the polymer when the polymer is in contact with the cell membrane it has a higher impact. *I.e.* the distribution of cationic charges within statistical or gradient copolymers could lead to an increased number of interactions with the cell membrane, thereby causing greater cytotoxicity. Such concept is presented visually in Fig. 7. Specifically, in can be observe that because the DMAEMA block coils many of the charges are not accessible to interact with the membrane. While when the cationic charges are more spread out in the polymer more charges are accessible to interact. Our results are also supported by the zeta potential values reported, where significant differences between block architectures and copolymers P5–P7 were found (Fig. 4).

5. Conclusions

In this study, the properties and cytotoxicity of seven DMAEMA-OEGMA300, linear copolymers were investigated for their suitability as potential delivery systems. Our results found statistical (or of statistical/tapered component) to cause a more overt reduction in cell viability than their block counterparts, suggesting that the monomer position in the polymer chain plays a key role in cytotoxicity. To the best of our knowledge this study is the first of its kind comparing the cytotoxicity of multiple linear architectures. Specifically, the toxicity was evaluated using MTT assay in a range of pancreatic cancer cell lines *versus* non-malignant control lines. While copolymers $OEGMA_{11}$-*b*-($OEGMA_9$-*co*-$DMAEMA_{18}$)-*b*-$DMAEMA_{21}$, a statistical-centre block, and $OEGMA_{10}$-*b*-($OEGMA_9$-*grad*-$DMAEMA_{15}$)-*b*-$DMAEMA_{22}$, a gradient, were found to significantly affect cell viability, it can be said that all polymers are well tolerated by these cell lines and in some cases metabolic activity increased that will need to be investigated further. We believe that OEGMA-DMAEMA copolymers have potential to overcome the cytotoxic limitations of bPEI and of PDMAEMA homopolymers and show promising properties as gene delivery systems to treat PDAC. Further studies on the delivery of therapeutic molecules by this copolymers and also how different factors like the composition affect toxicity will follow.

Conflicts of interest

There are no conflicts to declare.

Acknowledgements

The Engineering and Physical Sciences Research Council (EPSRC) and Department of Materials are acknowledged for the PhD studentships of J. S. C and B. S. The Medical Research Council (MRC) is acknowledged for the PhD studentship of S. M. B. T. K. G. would also like to thank the Royal Society of Chemistry for the RSC Enablement grant (E21-2117791382).

References

1 D. W. Pack, A. S. Hoffman, S. Pun and P. S. Stayton, Design and development of polymers for gene delivery, *Nat. Rev. Drug Discovery*, 2005, **4**, 581–593.
2 J. J. Green, R. Langer and D. G. Anderson, A Combinatorial Polymer Library Approach Yields Insight into Nonviral Gene Delivery, *Acc. Chem. Res.*, 2008, **41**, 749–759.
3 R. Kumar, *et al.*, Polymeric Delivery of Therapeutic Nucleic Acids, *Chem. Rev.*, 2021, **121**, 11527–11652.
4 A. C. Rinkenauer, S. Schubert, A. Traeger and U. S. Schubert, The influence of polymer architecture on in vitro pDNA transfection, *J. Mater. Chem. B*, 2015, **3**, 7477–7493.
5 F. J. Xu and W. T. Yang, Polymer vectors via controlled/living radical polymerization for gene delivery, *Prog. Polym. Sci.*, 2011, **36**, 1099–1131.
6 M. Ahmed and R. Narain, The effect of polymer architecture, composition, and molecular weight on the properties of glycopolymer-based non-viral gene delivery systems, *Biomaterials*, 2011, **32**, 5279–5290.
7 L. Parhamifar, *et al.*, Polycation-Mediated Integrated Cell Death Processes, *Adv. Genet.*, 2014, 353–398, DOI: **10.1016/B978-0-12-800148-6.00012-2**.
8 B. D. Monnery, *et al.*, Cytotoxicity of polycations: Relationship of molecular weight and the hydrolytic theory

of the mechanism of toxicity, *Int. J. Pharm.*, 2017, **521**, 249–258.
9 A. Verma and F. Stellacci, Effect of Surface Properties on Nanoparticleâ€“Cell Interactions, *Small*, 2010, **6**, 12–21.
10 U. Rungsardthong, *et al.*, Copolymers of amine methacrylate with poly(ethylene glycol) as vectors for gene therapy, *J. Controlled Release*, 2001, **73**, 359–380.
11 S. Agarwal, Y. Zhang, S. Maji and A. Greiner, PDMAEMA based gene delivery materials, *Mater. Today*, 2012, **15**, 388–393.
12 F. Danhier, *et al.*, PLGA-based nanoparticles: An overview of biomedical applications, *J. Controlled Release*, 2012, **161**, 505–522.
13 Z. Kadlecova, *et al.*, DNA delivery with hyperbranched polylysine: A comparative study with linear and dendritic polylysine, *J. Controlled Release*, 2013, **169**, 276–288.
14 P. Tarach and A. Janaszewska, Recent Advances in Preclinical Research Using PAMAM Dendrimers for Cancer Gene Therapy, *Int. J. Mol. Sci.*, 2021, **22**, 2912.
15 W. T. Godbey, K. K. Wu and A. G. Mikos, Poly(ethylenimine) and its role in gene delivery, *J. Controlled Release*, 1999, **60**, 149–160.
16 W. T. Godbey, K. K. Wu, G. J. Hirasaki and A. G. Mikos, Improved packing of poly(ethylenimine)/DNA complexes increases transfection efficiency, *Gene Ther.*, 1999, **6**, 1380–1388.
17 W. T. Godbey, K. K. Wu and A. G. Mikos, Tracking the intracellular path of poly(ethylenimine)/DNA complexes for gene delivery, *Proc. Natl. Acad. Sci. U. S. A.*, 1999, **96**, 5177–5181.
18 W. T. Godbey, M. A. Barry, P. Saggau, K. K. Wu and A. G. Mikos, Poly(ethylenimine)-mediated transfection: A new paradigm for gene delivery, *J. Biomed. Mater. Res.*, 2000, **51**, 321–328.
19 D. Fischer, Y. Li, B. Ahlemeyer, J. Krieglstein and T. Kissel, In vitro cytotoxicity testing of polycations: influence of polymer structure on cell viability and hemolysis, *Biomaterials*, 2003, **24**, 1121–1131.
20 E. Haladjova, *et al.*, Physicochemical Properties and Biological Performance of Polymethacrylate Based Gene Delivery Vector Systems: Influence of Amino Functionalities, *Macromol. Biosci.*, 2021, **21**, 2000352.
21 M. C. Deshpande, *et al.*, Influence of polymer architecture on the structure of complexes formed by PEG–tertiary amine methacrylate copolymers and phosphorothioate oligonucleotide, *J. Controlled Release*, 2002, **81**, 185–199.
22 A. B. Cook, *et al.*, Cationic and hydrolysable branched polymers by RAFT for complexation and controlled release of dsRNA, *Polym. Chem.*, 2018, **9**, 4025–4035.
23 D. Sprouse and T. M. Reineke, Investigating the Effects of Block versus Statistical Glycopolycations Containing Primary and Tertiary Amines for Plasmid DNA Delivery, *Biomacromolecules*, 2014, **15**, 2616–2628.
24 B. Mendrek, *et al.*, Synthesis, Characterization and Cytotoxicity of Novel Thermoresponsive Star Copolymers of N,N′-Dimethylaminoethyl Methacrylate and Hydroxyl-Bearing Oligo(Ethylene Glycol) Methacrylate, *Polymers*, 2018, **10**, 1255.
25 B. Mendrek, *et al.*, Nonviral Plasmid DNA Carriers Based on N, N ′-Dimethylaminoethyl Methacrylate and Di(ethylene glycol) Methyl Ether Methacrylate Star Copolymers, *Biomacromolecules*, 2015, **16**, 3275–3285.
26 J.-F. Lutz, Polymerization of oligo(ethylene glycol) (meth) acrylates: Toward new generations of smart biocompatible materials, *J. Polym. Sci., Part A: Polym. Chem.*, 2008, **46**, 3459–3470.
27 V. V. Khutoryanskiy, Beyond PEGylation: Alternative surface-modification of nanoparticles with mucus-inert biomaterials, *Adv. Drug Delivery Rev.*, 2018, **124**, 140–149.
28 S. Venkataraman, *et al.*, The role of PEG architecture and molecular weight in the gene transfection performance of PEGylated poly(dimethylaminoethyl methacrylate) based cationic polymers, *Biomaterials*, 2011, **32**, 2369–2378.
29 C. E. Nelson, *et al.*, Balancing cationic and hydrophobic content of PEGylated siRNA polyplexes enhances endosome escape, stability, blood circulation time, and bioactivity in vivo, *ACS Nano*, 2013, **7**, 8870–8880.
30 M. Le Bohec, *et al.*, Structure-pDNA complexation and structure–cytotoxicity relationships of PEGylated, cationic aminoethyl-based polyacrylates with tunable topologies, *Polym. Chem.*, 2019, **10**, 1968–1977.
31 D. Santo, *et al.*, Poly(ethylene glycol)- block -poly(2-aminoethyl methacrylate hydrochloride)-Based Polyplexes as Serum-Tolerant Nanosystems for Enhanced Gene Delivery, *Mol. Pharm.*, 2019, **16**, 2129–2141.
32 L. L. Tayo, *et al.*, Design of hemocompatible poly (DMAEMA-*co*-PEGMA) hydrogels for controlled release of insulin, *J. Appl. Polym. Sci.*, 2015, **132**, 1–12.
33 A. Frère, *et al.*, PEGylated and Functionalized Aliphatic Polycarbonate Polyplex Nanoparticles for Intravenous Administration of HDAC5 siRNA in Cancer Therapy, *ACS Appl. Mater. Interfaces*, 2017, **9**, 2181–2195.
34 W. T. Godbey, K. K. Wu and A. G. Mikos, Size matters: Molecular weight affects the efficiency of poly(ethylenimine) as a gene delivery vehicle, *J. Biomed. Mater. Res.*, 1999, **45**, 268–275.
35 J. Cai, *et al.*, Effect of Chain Length on Cytotoxicity and Endocytosis of Cationic Polymers, *Macromolecules*, 2011, **44**, 2050–2057.
36 T. K. Georgiou, M. Vamvakaki, C. S. Patrickios, E. N. Yamasaki and L. A. Phylactou, Nanoscopic Cationic Methacrylate Star Homopolymers: Synthesis by Group Transfer Polymerization, Characterization and Evaluation as Transfection Reagents, *Biomacromolecules*, 2004, **5**, 2221–2229.
37 T. K. Georgiou, M. Vamvakaki, L. A. Phylactou and C. S. Patrickios, Synthesis, Characterization, and Evaluation as Transfection Reagents of Double-Hydrophilic Star Copolymers: Effect of Star Architecture, *Biomacromolecules*, 2005, **6**, 2990–2997.

38 T. K. Georgiou, Star polymers for gene delivery, *Polym. Int.*, 2014, **63**, 1130–1133.
39 A. B. Cook and S. Perrier, Branched and Dendritic Polymer Architectures: Functional Nanomaterials for Therapeutic Delivery, *Adv. Funct. Mater.*, 2019, **1901001**, 1–24.
40 T. J. Gibson, *et al.*, Star polymers with acid-labile diacetal-based cores synthesized by aqueous RAFT polymerization for intracellular DNA delivery, *Polym. Chem.*, 2020, **11**, 344–357.
41 A. Fus-Kujawa, *et al.*, Functional star polymers as reagents for efficient nucleic acids delivery into HT-1080 cells, *Int. J. Polym. Mater. Polym. Biomater.*, 2020, 1–15, DOI: 10.1080/00914037.2020.1716227.
42 R. Whitfield, *et al.*, Efficient Binding, Protection, and Self-Release of dsRNA in Soil by Linear and Star Cationic Polymers, *ACS Macro Lett.*, 2018, **7**, 909–915.
43 J. M. Rabanel, *et al.*, Effect of polymer architecture on curcumin encapsulation and release from PEGylated polymer nanoparticles: Toward a drug delivery nano-platform to the CNS, *Eur. J. Pharm. Biopharm.*, 2015, **96**, 409–420.
44 A. B. Cook, *et al.*, Hyperbranched poly(ethylenimine- co -oxazoline) by thiol–yne chemistry for non-viral gene delivery: investigating the role of polymer architecture, *Polym. Chem.*, 2019, **10**, 1202–1212.
45 T. Bus, *et al.*, 3rd generation poly(ethylene imine)s for gene delivery, *J. Mater. Chem. B*, 2017, **5**, 1258–1274.
46 A. M. Alhoranta, *et al.*, Cationic amphiphilic star and linear block copolymers: synthesis, self-assembly, and in vitro gene transfection, *Biomacromolecules*, 2011, **12**, 3213–3222.
47 C. Cheng, A. J. Convertine, P. S. Stayton and J. D. Bryers, Multifunctional triblock copolymers for intracellular messenger RNA delivery, *Biomaterials*, 2012, **33**, 6868–6876.
48 J. Moraes, *et al.*, Influence of Block versus Random Monomer Distribution on the Cellular Uptake of Hydrophilic Copolymers, *ACS Macro Lett.*, 2016, **5**, 1416–1420.
49 S. Lin, *et al.*, An Acid-Labile Block Copolymer of PDMAEMA and PEG as Potential Carrier for Intelligent Gene Delivery Systems, *Biomacromolecules*, 2008, **9**, 109–115.
50 A. Schallon, *et al.*, Performance of three PDMAEMA-based polycation architectures as gene delivery agents in comparison to linear and branched PEI, *React. Funct. Polym.*, 2010, **70**, 1–10.
51 M. Vamvakaki, N. C. Billingham and S. P. Armes, Synthesis of water-soluble statistical copolymers and terpolymers containing pendent oligo(ethylene glycol derivatives), *Polymer*, 1999, **40**, 5161–5171.
52 I. B. Dicker, *et al.*, Oxyanions catalyze group-transfer polymerization to give living polymers, *Macromolecules*, 1990, **23**, 4034–4041.
53 P. Hiemenz, *Polymer Chemistry: Basic Concepts*, Marcel Dekker, 1984.
54 Q. Li, L. Wang, F. Chen, A. Constantinou and T. K. Georgiou, Thermoresponsive Oligo(ethylene glycol) Methyl Ether Methacrylate based Copolymers: Composition and Comonomer Effect, *Polym. Chem.*, 2022, **13**, 2506–2518.
55 M. A. Ward and T. K. Georgiou, Thermoresponsive terpolymers based on methacrylate monomers: Effect of architecture and composition, *J. Polym. Sci., Part A: Polym. Chem.*, 2010, **48**, 775–783.
56 A. P. Constantinou, N. F. Sam-Soon, D. R. Carroll and T. K. Georgiou, Thermoresponsive Tetrablock Terpolymers: Effect of Architecture and Composition on Gelling Behavior, *Macromolecules*, 2018, **51**, 7019–7031.
57 A. P. Constantinou, K. Zhang, B. Somuncuoğlu, B. Feng and T. K. Georgiou, PEG-Based Methacrylate Tetrablock Terpolymers: How Does the Architecture Control the Gelation?, *Macromolecules*, 2021, **54**, 6511–6524.
58 A. P. Constantinou, N. Provatakis, Q. Li and T. K. Georgiou, Homopolymer and ABC Triblock Copolymer Mixtures for Thermoresponsive Gel Formulations, *Gels*, 2021, **7**, 116.
59 A. P. Constantinou, A. Tall, Q. Li and T. K. Georgiou, Liquid–liquid phase separation in aqueous solutions of poly(ethylene glycol) methacrylate homopolymers, *J. Polym. Sci.*, 2022, **60**, 188–198.
60 Q. Li, A. P. Constantinou and T. K. Georgiou, A library of thermoresponsive PEG –based methacrylate homopolymers: How do the molar mass and number of ethylene glycol groups affect the cloud point?, *J. Polym. Sci.*, 2021, **59**, 230–239.
61 V. Bütün, S. Armes and N. Billingham, Synthesis and aqueous solution properties of near-monodisperse tertiary amine methacrylate homopolymers and diblock copolymers, *Polymer*, 2001, **42**, 5993–6008.
62 D. E. Zhunuspayev, G. A. Mun and V. V. Khutoryanskiy, Temperature-Responsive Properties and Drug Solubilization Capacity of Amphiphilic Copolymers Based on N -Vinylpyrrolidone and Vinyl Propyl Ether, *Langmuir*, 2010, **26**, 7590–7597.
63 M. A. Ward and T. K. Georgiou, Thermoresponsive triblock copolymers based on methacrylate monomers: effect of molecular weight and composition, *Soft Matter*, 2012, **8**, 2737.
64 A. P. Constantinou, B. Zhan and T. K. Georgiou, Tuning the Gelation of Thermoresponsive Gels Based on Triblock Terpolymers, *Macromolecules*, 2021, **54**, 1943–1960.
65 D. Fournier, R. Hoogenboom, H. M. L. Thijs, R. M. Paulus and U. S. Schubert, Tunable pH- and Temperature-Sensitive Copolymer Libraries by Reversible Addition−Fragmentation Chain Transfer Copolymerizations of Methacrylates, *Macromolecules*, 2007, **40**, 915–920.
66 C. Pietsch, *et al.*, Thermo-Induced Self-Assembly of Responsive Poly(DMAEMA- b -DEGMA) Block Copolymers into Multi- and Unilamellar Vesicles, *Macromolecules*, 2012, **45**, 9292–9302.
67 J. H. Tan, *et al.*, Hyperbranched polymers as delivery vectors for oligonucleotides, *J. Polym. Sci., Part A: Polym. Chem.*, 2012, **50**, 2585–2595.
68 P. van de Wetering, N. M. E. Schuurmans-Nieuwenbroek, M. J. van Steenbergen, D. J. A. Crommelin and W. E. Hennink, Copolymers of 2-(dimethylamino)ethyl

methacrylate with ethoxytriethylene glycol methacrylate or N-vinyl-pyrrolidone as gene transfer agents, *J. Controlled Release*, 2000, **64**, 193–203.

69 B. Somuncuoğlu, Y. L. Lee, A. P. Constantinou, D. L. M. Poussin and T. K. Georgiou, Ethyl methacrylate diblock copolymers as polymeric surfactants: Effect of molar mass and composition, *Eur. Polym. J.*, 2021, **154**, 110537.

70 P. Patel, N. M. Ibrahim and K. Cheng, The Importance of Apparent pKa in the Development of Nanoparticles Encapsulating siRNA and mRNA, *Trends Pharmacol. Sci.*, 2021, **42**, 448–460.

71 S. Bhattacharjee, DLS and zeta potential – What they are and what they are not?, *J. Controlled Release*, 2016, **235**, 337–351.

72 A. Venault, *et al.*, Tunable PEGylation of branch-type PEI/DNA polyplexes with a compromise of low cytotoxicity and high transgene expression: in vitro and in vivo gene delivery, *J. Mater. Chem. B*, 2017, **5**, 4732–4744.

73 B. Yu, Reducible Poly (2-Dimethylaminoethyl) Methacrylate-Block-Polyvinylimidazole: Synthesis, Transfection Activity in Vitro, *J. Biomater. Nanobiotechnol.*, 2012, **03**, 118–124.

74 D. B. Bitoque, *et al.*, Efficiency of RAFT-synthesized PDMAEMA in gene transfer to the retina, *J. Tissue Eng. Regener. Med.*, 2017, **11**, 265–275.

75 A. Burgess, M. Rasouli and S. Rogers, Stressing Mitosis to Death, *Front. Oncol.*, 2014, **4**, 81–87.

76 S. Fulda, A. M. Gorman, O. Hori and A. Samali, Cellular Stress Responses: Cell Survival and Cell Death, *Int. J. Cell Biol.*, 2010, **2010**, 1–23.

77 E. L. Deer, *et al.*, Phenotype and Genotype of Pancreatic Cancer Cell Lines, *Pancreas*, 2010, **39**, 425–435.

78 S. Ottaviani, *et al.*, TGF-β induces miR-100 and miR-125b but blocks let-7a through LIN28B controlling PDAC progression, *Nat. Commun.*, 2018, **9**, 1845.

79 M. Orth, *et al.*, Pancreatic ductal adenocarcinoma: biological hallmarks, current status, and future perspectives of combined modality treatment approaches, *Radiat. Oncol.*, 2019, **14**, 141.

80 M. Breunig, U. Lungwitz, R. Liebl and A. Goepferich, Breaking up the correlation between efficacy and toxicity for nonviral gene delivery, *Proc. Natl. Acad. Sci. U. S. A.*, 2007, **104**, 14454–14459.

81 P. Bhoopathi, *et al.*, Pancreatic Cancer–Specific Cell Death Induced In Vivo by Cytoplasmic-Delivered Polyinosine–Polycytidylic Acid, *Cancer Res.*, 2014, **74**, 6224–6235.

82 V. Kafil and Y. Omidi, Cytotoxic Impacts of Linear and Branched Polyethylenimine Nanostructures in A431 Cells, *Bioimpacts*, 2011, **1**(1), 23–30.

83 A. P. Constantinou, *et al.*, Investigation of the Thermogelation of a Promising Biocompatible ABC Triblock Terpolymer and Its Comparison with Pluronic F127, *Macromolecules*, 2022, **55**, 1783–1799.

84 S. M. Moghimi, *et al.*, A two-stage poly(ethylenimine)-mediated cytotoxicity: implications for gene transfer/therapy, *Mol. Ther.*, 2005, **11**, 990–995.

85 P. Singhsa, D. Diaz-Dussan, H. Manuspiya and R. Narain, Well-Defined Cationic N -[3-(Dimethylamino)propyl]methacrylamide Hydrochloride-Based (Co)polymers for siRNA Delivery, *Biomacromolecules*, 2018, **19**, 209–221.

86 R. A. Cordeiro, *et al.*, High transfection efficiency promoted by tailor-made cationic tri-block copolymer-based nanoparticles, *Acta Biomater.*, 2017, **47**, 113–123.

87 D. Santo, *et al.*, Combination of Poly[(2-dimethylamino) ethyl methacrylate] and Poly(β-amino ester) Results in a Strong and Synergistic Transfection Activity, *Biomacromolecules*, 2017, **18**, 3331–3342.

88 J. P. Bost, *et al.*, Delivery of Oligonucleotide Therapeutics: Chemical Modifications, Lipid Nanoparticles, and Extracellular Vesicles, *ACS Nano*, 2021, **15**, 13993–14021.

89 P. Ruenraroengsak, *et al.*, Respiratory epithelial cytotoxicity and membrane damage (holes) caused by amine-modified nanoparticles, *Nanotoxicology*, 2012, **6**, 94–108.